Scientific paper

Synthesis and Biological Evaluation of Some Hydrazide-Hydrazone Derivatives as Anticancer Agents

Kadriye Akdağ,[1] Fatih Tok,[1] Sevgi Karakuş,[1,*] Ömer Erdoğan,[2] Özge Çevik[2] and Bedia Koçyiğit-Kaymakçıoğlu[1]

[1] *Department of Pharmaceutical Chemistry, Faculty of Pharmacy, Marmara University, 34854, Istanbul, Turkey*

[2] *Department of Biochemistry, School of Medicine, Aydin Adnan Menderes University, 09010, Aydın, Turkey*

* *Corresponding author: E-mail: skarakus@marmara.edu.tr*

Received: 10-04-2022

Abstract

In this study, a series of hydrazide-hydrazone derivatives (**3a**-**3u**) were synthesized and evaluated for their anticancer activities against prostate cancer cell line (PC-3), breast cancer cell line (MCF-7), colon cancer cell line (HT-29) and human umbilical vein endothelial cells (HUVEC) using MTT assay. In particular, compound **3h** having a pyrrole ring was found to be the most potent derivative with IC_{50} = 1.3, 3.0, 1.7 μM against PC-3, MCF-7, HT-29 cancer cell lines respectively using paclitaxel as a standard compound. Furthermore, compound **3h** was subjected to further biological studies such as caspase-3 activity and Annexin-V assay to evaluate their inhibitory potentials. The activity results displayed that compound **3h** increased caspase-3 activation and the number of cells to early apoptosis. The additional studies like pharmacokinetics, bioavailability scores and drug-likeness properties were also evaluated. The *in silico* pharmacokinetics predictions displayed that the bioavailability of these compounds may be high.

Keywords: Hydrazone, anticancer, apoptosis, drug-likeness, MCF-7.

1. Introduction

Cancer is a disease characterized by the uncontrolled proliferation and spread of the body's cells. It is the second leading cause of death in developed countries after cardiovascular diseases. It was reported that one out of every two people born after 1960 will get cancer. The distribution of cancer types according to gender differs.[1]

While breast cancer is more common in women than other types of cancer, prostate cancer is more common in men. Lung cancer and colorectal cancer highly affect both men and women.[2] There are different approaches to cancer treatment such as surgery, radiotherapy, chemotherapy and hormone therapy. Despite their severe toxicity, chemotherapy is the main approach for the treatment of cancer worldwide.[3] Detailed analyses of pathways and mechanisms and structures of antitumor compounds have led to significant developments in the prevention and treatment of cancer. Therefore, there is still a need for new anticancer compounds with higher potency and less toxicity, as well as less toxic to non-cancerous cells.[4]

Researchers working in the field of discovering new drugs seek to synthesize simple compounds having various pharmacological activities such as anticancer, antiviral, antibacterial, antioxidant.[5] Hydrazide-hydrazone derivatives are molecules containing a highly reactive group (CO-NH-N=CH) and are considered to be a good candidate for the development of a new drug.[6-8]

There are many studies in the literature that hydrazide-hydrazones have anticancer activity. Saini *et. al.* presented useful information about the mechanisms of anticancer activity of hydrazide-hydrazones.[9] Hydrazone structures can act by inhibiting topoisomerases, protein kinases and induce apoptosis pathways.[10,11] Abou-Seri *et al.* designed and synthesized potent hydrazones as potential inhibitors of VEGFR2.[12] Taha *et al.* synthesized a new morpholine hydrazone scaffold due to potential anticancer activity.[13] In addition, the benzothiazole-hydrazone derivatives were reported as potent anticancer agents.[14] In another study, the hydrazone derivatives bearing the pyridine ring synthesized and assessed the anticancer activity against MCF-7. In this study, some of the tested compounds displayed higher anticancer activity than cisplatin.[15] Hydrazone structures play an important role in anticancer-related processes, as mentioned in the examples above.

In light of the above information, we synthesized some hydrazone derivatives and investigated them for their anticancer activity against prostate cancer cell line (PC-3), breast cancer cell line (MCF-7), colon cancer cell line (HT-29) and human umbilical vein endothelial cells (HUVEC).

2. Experimental

All chemicals were purchased from Merck Company and Sigma-Aldrich. Melting points were determined by using a SMP II melting point apparatus. IR spectra were recorded on a Shimadzu FTIR-8400S spectrophotometer. ^{1}H-NMR and ^{13}C-NMR spectra were obtained on a Bruker Avance DPX-400 spectrometer. Tetramethylsilane as the internal standard and DMSO-d_6 as the solvent was used for NMR spectrums. Elemental analyses were performed with GmbH varioMICRO CHNS.

2. 1. Synthesis

2. 1. 1. General procedure for the synthesis of ethyl 4-[(4-methoxybenzoyl)amino] benzoate (1)

Ethyl 4-aminobenzoate (1mmol) was dissolved in ether (10 mL). 1 mmol of 4-methoxybenzoyl chloride was added dropwise to this solution. It was stirred for 2 hours on a magnetic stirrer. The precipitate was washed with water, filtered and dried.[16]

2. 1. 2. General procedure for the synthesis of *N*-[4-(hydrazinylcarbonyl)phenyl]-4-methoxybenzamide (2)

Ethyl 4-[(4-methoxybenzoyl)amino]benzoate (1 mmol) was heated with hydrazine monohydrate (3 mL) in ethanol (15 mL) for 10 hours at 100 °C. After TLC control, the precipitate was filtered and crystallized with ethanol.[16]

2. 1. 3. General procedure for the synthesis of hydrazide-hydrazones (3a-3u)

In a solution of *N*-(4-(hydrazinecarbonyl)phenyl)-4-methoxybenzamide (1 mmol) in 10 mL ethanol was added 1 mmol substituted aldehyde derivatives. The mixture was refluxed for 8 hours. After TLC control, the precipitate was filtered and dried. The product was crystallized with ethanol.[17] Compounds **3j**, **3l**, **3m**, **3n**, **3r** and **3u** were reported in the literature.[18-20] The other hydrazone derivatives were synthesized for the first time in this article.

***N*-{4-[2-(2,4-Dichlorobenzylidene)hydrazinecarbonyl] phenyl}-4-methoxybenzamide (3a)**

Yield: 68%, M.p. = 298-299 °C, FTIR (ν, cm^{-1}): 3271, 3173 (N-H), 3010 (=C-H), 2983 (C-H), 1641 (C=O), 1606 (C=N), 1589, 1444 (C=C), 852 (=C-H). ^{1}H-NMR (400 MHz, DMSO-d_6, ppm): δ 3.85 (s, 3H, OCH_3), 7.07-8.04 (m, 11H, Ar-H), 8.83 (s, 1H, =CH-), 10.37 (s, 1H, -CONH-), 12.08 (s, 1H, -CONHN=). ^{13}C-NMR (100 MHz, DMSO-d_6, ppm): δ 55.44 (OCH_3), 113.66, 119.42, 126.56, 128.00, 128.48, 129.35, 129.74, 130.80, 133.76, 134.94, 142.09, 142.80, 162.12, 162.59 (C=O), 165.18 (C=O). Anal. Calcd for $C_{22}H_{17}Cl_2N_3O_3$: C 59.74, H 3.87, N 9.50. Found: C 59.56, H 3.90, N 9.42 %.

***N*-(4-(2-(3,4-Dichlorobenzylidene)hydrazinecarbonyl) phenyl)-4-methoxybenzamide (3b)**

Yield: 63%, M.p. = 280-281 °C, FTIR (ν, cm^{-1}): 3315, 3238 (N-H), 3072 (=C-H), 2935 (C-H), 1641 (C=O), 1602 (C=N), 1589, 1543 (C=C), 840 (=C-H). ^{1}H-NMR (400 MHz, DMSO-d_6, ppm): δ 3.83 (s, 3H, OCH_3), 7.05–7.98 (m, 11H, Ar-H), 8.41 (s, 1H, =CH-), 10.34 (s, 1H, -CONH-), 11.95 (s, 1H, -CONHN=). ^{13}C-NMR (100 MHz, DMSO-d_6, ppm): δ 55.44 (OCH_3), 113.64, 119.41, 126.56, 127.49, 129.74, 131.07, 131.69, 132.09, 135.28, 142.73, 144.52, 162.10, 162.71 (C=O), 165.17 (C=O). Anal. Calcd for $C_{22}H_{17}Cl_2N_3O_3$: C 59.74, H 3.87, N 9.50. Found: C 59.49, H 3.91, N 9.44 %.

***N*-{4-[2-(4-Nitrobenzylidene)hydrazinecarbonyl]phenyl}-4-methoxybenzamide (3c)**

Yield: 57%, M.p. = 334-335 °C, FTIR (ν, cm^{-1}): 3302, 3213 (N-H), 3068 (=C-H), 2837 (C-H), 1643 (C=O), 1602 (C=N), 1587, 1537 (C=C), 833 (=C-H). ^{1}H-NMR (400 MHz, DMSO-d_6, ppm): δ 3.85 (s, 3H, OCH_3), 7.07-8.33 (m, 12H, Ar-H), 8.56 (s, 1H, =CH-), 10.41 (s, 1H, -CONH-), 12.09 (s, 1H, -CONHN=). ^{13}C-NMR (100 MHz, DMSO-d_6, ppm): δ 55.91 (OCH_3), 114.11, 119.87, 124.52, 127.00, 128.35, 128.99, 130.20, 141.21, 148.21, 162.57 (C=O), 165.63 (C=O). Anal. Calcd for $C_{22}H_{18}N_4O_5$: C 63.15, H 4.34, N 13.39. Found: C 62.96, H 4.33, N 13.31 %.

***N*-{4-[2-(3-Nitrobenzylidene)hydrazinecarbonyl]phenyl}4-methoxybenzamide (3d)**

Yield: 58%, M.p. = 294 °C, FTIR (ν, cm^{-1}): 3302, 3228 (N-H), 3074 (=C-H), 2845 (C-H), 1637 (C=O), 1602 (C=N), 1525, 1506 (C=C), 842 (=C-H). ^{1}H-NMR (400 MHz, DMSO-d_6, ppm): δ 3.83 (s, 3H, OCH_3), 7.04–8.26 (m, 12H, Ar-H), 8.54 (s, 1H, =CH-), 10.35 (s, 1H, -CONH-), 12.04 (s, 1H, -CONHN=). ^{13}C-NMR (100 MHz, DMSO-d_6, ppm): δ 55.44 (OCH_3), 113.65, 119.41, 120.80, 124.11, 126.55, 128.51, 129.75, 130.43, 133.32, 136.30, 142.76, 144.83, 148.23, 162.11, 162.77 (C=O), 165.17 (C=O). Anal. Calcd for $C_{22}H_{18}N_4O_5$: C 63.15, H 4.34, N 13.39. Found: C 62.99, H 4.35, N 13.33 %.

***N*-{4-[2-(3,5-Dichloro-2-hydroxybenzylidene)hydrazinecarbonyl]phenyl}-4-methoxybenzamide (3e)**

Yield: 61.%, M.p. = 331-332 °C, FTIR (ν, cm^{-1}): 3340, 3219 (N-H), 3039 (=C-H), 2970 (C-H), 1645 (C=O), 1602 (C=N), 1587, 1500 (C=C), 840 (=C-H). ^{1}H-NMR

(400 MHz, DMSO-d_6, ppm): δ 3.86 (s, 3H, OCH_3), 7.08-8.01 (m, 10H, Ar-H), 8.58 (s, 1H, =CH-), 10.40 (s, 1H, -CONH-), 12.26 (s, 1H, -CONHN=), 12.83 (s, 1H, OH). ^{13}C-NMR (100 MHz, DMSO-d_6, ppm): δ 55.44 (OCH_3), 113.66, 119.41, 126.55, 127.37, 128.01, 128.47, 129.74, 130.80, 133.76, 142.09, 142.79, 162.11, 162.57 (C=O), 165.17 (C=O). Anal. Calcd for $C_{22}H_{17}Cl_2N_3O_4$: C 57.66, H 3.74, N 9.17. Found: C 57.47, H 3.75, N 9.14 %.

***N*-{4-[2-(Pyridine-4-ylmethylene)hydrazinecarbonyl] phenyl}-4-methoxybenzamide (3f)**

Yield: 75%, M.p. = 311-312 °C, FTIR (ν, cm^{-1}): 3327, 3263 (N-H), 3032 (=C-H), 2910 (C-H), 1645 (C=O), 1602 (C=N), 1525, 1496 (C=C), 842 (=C-H). ^{1}H-NMR (400 MHz, DMSO-d_6, ppm): δ 3.85 (s, 3H, OCH_3), 7.08-8.65 (m, 12H, Ar-H), 8.67 (s, 1H, =CH-), 10.38 (s, 1H, -CONH-), 12.06 (s, 1H, -CONHN=). ^{13}C-NMR (100 MHz, DMSO-d_6, ppm): δ 55.49 (OCH_3), 113.70, 119.45, 120.98, 126.56, 128.59, 129.80, 141.60, 142.88, 144.85, 150.31, 162.15, 162.82 (C=O), 165.24 (C=O). Anal. Calcd for $C_{21}H_{18}N_4O_3$: C 67.37, H 4.85, N 14.96. Found: C 67.14, H 4.82, N 14.94 %.

***N*-{4-[2-(Pyridine-3-ylmethylene)hydrazinecarbonyl] phenyl}-4-methoxybenzamide (3g)**

Yield: 65%, M.p. = 287 °C, FTIR (ν, cm^{-1}): 3336, 3273 (N-H), 3043 (=C-H), 2982 (C-H), 1647 (C=O), 1602 (C=N), 1589, 1471 (C=C), 844 (=C-H). ^{1}H-NMR (400 MHz, DMSO-d_6, ppm): δ 3.85 (s, 3H, OCH_3), 7.07–8.62 (m, 12H, Ar-H), 8.86 (s, 1H, =CH-), 10.37 (s, 1H, -CONH-), 11.96 (s, 1H, -CONHN=). ^{13}C-NMR (100 MHz, DMSO-d_6, ppm): δ 55.49 (OCH_3), 113.70, 119.46, 124.06, 126.58, 128.49, 129.79, 130.35, 133.41, 142.73, 144.57, 148.73, 150.66, 162.14, 162.67 (C=O), 165.21 (C=O). Anal. Calcd for $C_{21}H_{18}N_4O_3$: C 67.37, H 4.85, N 14.96. Found: C 67.07, H 4.83, N 14.92 %.

***N*-{4-[2-(1*H*-Pyrrol-3-yl-methylene)hydrazinecarbonyl]phenyl}-4-methoxybenzamide (3h)**

Yield: 78%, M.p. = 273 °C, FTIR (ν, cm^{-1}): 3308, 3194 (N-H), 3047 (=C-H), 2964 (C-H), 1645 (C=O), 1604 (C=N), 1525, 1500 (C=C), 842 (=C-H). ^{1}H-NMR (400 MHz, DMSO-d_6, ppm): δ 3.83 (s, 3H, OCH_3),4.65 (s, 1H, NH), 7.11-7.87 (m, 11H, Ar-H), 8.33 (s, 1H, =CH-), 10.28 (s, 1H, -CONH-), 11.65 (s, 1H, -CONHN=).^{13}C-NMR (100 MHz, DMSO-d_6, ppm): δ 55.48 (OCH_3), 113.67, 119.39, 126.69, 127.60, 127.91, 129.74, 141.91, 162.07, 165.15 (C=O), 165.57 (C=O). Anal. Calcd for $C_{20}H_{18}N_4O_3$: C 66.29, H 5.01, N 15.46. Found: C 66.17, H 5.04, N 15.39 %.

***N*-{4-[2-(Thiophen-2-ylmethylene)hydrazinecarbonyl] phenyl}-4-methoxybenzamide (3i)**

Yield: 70%, M.p. = 250-251 °C, FTIR (ν, cm^{-1}): 3304, 3192 (N-H), 3012 (=C-H), 2966 (C-H), 1645 (C=O), 1604 (C=N), 1581, 1491 (C=C), 842 (=C-H). ^{1}H-NMR (400 MHz, DMSO-d_6, ppm): δ 3.82 (s, 3H, OCH_3), 7.04–7.97 (m, 11H, Ar-H), 8.41 (s, 1H, =CH-), 10.32 (s, 1H, -CONH-), 11.79 (s, 1H, -CONHN=). ^{13}C-NMR (100 MHz, DMSO-d_6, ppm): δ 55.36 (OCH_3), 113.56, 119.32, 126.46, 127.75, 128.23, 128.73, 129.65, 130.68, 139.13, 142.37, 161.99, 162.30 (C=O), 165.06 (C=O). Anal. Calcd for $C_{20}H_{17}N_3O_3S$: C 63.31, H 4.52, N 11.07. Found: C 63.40, H 4.53, N 11.13 %.

***N*-{4-[2-(5-Nitrofuran-2-yl-methylene)hydrazinecarbonyl]phenyl}-4-methoxybenzamide (3j)**

Yield: 64%, M.p. = 297-298°C. Ref. lit. M.p= 292 °C.[18]

***N*-{4-[2-(2-Chloroquinolin-3-yl-methylene)hydrazinecarbonyl]phenyl}-4-methoxybenzamide (3k)**

Yield: 58%, M.p. = 302 °C, FTIR (ν, cm^{-1}): 3281, 3227 (N-H), 3030 (=C-H), 2989 (C-H), 1641 (C=O), 1604 (C=N), 1591, 1537 (C=C), 840 (=C-H). ^{1}H-NMR (400 MHz, DMSO-d_6, ppm): δ 3.86 (s, 3H, OCH_3), 7.08–8.26 (m, 13H, Ar-H), 8.94 (s, 1H, =CH-), 10.39 (s, 1H, -CONH-), 12.21 (s, 1H, -CONHN=). ^{13}C-NMR (100 MHz, DMSO-d_6, ppm): δ 55.36 (OCH_3), 113.57, 119.34, 126.16, 126.44, 126.80, 127.24, 127.53, 127.76, 128.47, 128.92, 129.67, 131.65, 135.49, 142.22, 142.77, 147.01, 148.41, 162.03, 162.55 (C=O), 165.09 (C=O). Anal. Calcd for $C_{25}H_{19}ClN_4O_3$: C 65.43, H 4.17, N 12.21. Found: C 65.29, H 4.21, N 12.14 %.

***N*-[4-(2-Benzylidenehydrazinecarbonyl)phenyl]-4-methoxybenzamide (3l)**

Yield: 65%, M.p. = 292-293 °C. Ref. lit. M.p = 282 °C.[19]

***N*-{4-[2-(4-Hydroxybenzylidene)hydrazinecarbonyl] phenyl}-4-methoxybenzamide (3m)**

Yield: 78%, M.p. = 284-285 °C. Ref. lit. M.p= 289 °C.[19]

***N*-{4-[2-(4-Hydroxy-3-methoxybenzylidene)hydrazinecarbonyl]phenyl}-4-methoxybenzamide (3n)**

Yield: 67%, M.p. = 264-265 °C. Ref. lit. M.p= 270 °C.[19]

***N*-{4-[2-(3-(4-Chlorophenoxybenzylidene)hydrazinecarbonyl]phenyl}-4-methoxybenzamide (3o)**

Yield: 74%, M.p. = 252-253 °C, FTIR (ν, cm^{-1}): 3329, 3259 (N-H), 3005 (=C-H), 2837 (C-H), 1641 (C=O), 1604 (C=N), 1573, 1508 (C=C), 839 (=C-H). ^{1}H-NMR (400 MHz, DMSO-d_6, ppm): δ 3.82 (s, 3H, OCH_3), 7.04-7.97 (m, 16H, Ar-H), 8.42 (s, 1H, =CH-), 10.33 (s, 1H, -CONH-), 11.81 (s, 1H, -CONHN=). ^{13}C-NMR (100 MHz, DMSO-d_6, ppm): δ 55.35 (OCH_3), 113.56, 115.85, 119.31, 120.44, 122.95, 126.46, 127.44, 128.31, 129.66, 129.92, 130.60, 136.48, 142.56, 146.35, 155.23, 156.71, 162.00, 162.48 (C=O), 165.07 (C=O). Anal. Calcd for $C_{28}H_{22}ClN_3O_4$: C 67.27, H 4.44, N 8.40. Found: C 67.15, H 4.42, N 8.36 %.

***N*-{4-[2-(2-Phenylethylidene)hydrazinecarbonyl]phenyl}-4-methoxybenzamide (3p)**

Yield: 68%, M.p. = 305-306 °C, FTIR (ν, cm^{-1}): 3296, 3223 (N-H), 3037 (=C-H), 2841 (C-H), 1651 (C=O), 1602 (C=N), 1548, 1504 (C=C), 840 (=C-H). ^{1}H-NMR

(400 MHz, DMSO-d_6, ppm): δ 3.60 (d, 2H, -CH_2), 3.82 (s, 3H, OCH_3), 7.04-8.02 (m, 13H, Ar-H), 8.42 (s, 1H, =CH-), 10.29 (s, 1H, -CONH-), 11.47 (s, 1H, -CONHN=). ^{13}C-NMR (100 MHz, DMSO-d_6, ppm): δ 55.37 (OCH_3), 113.55, 119.27, 125.73, 126.52, 127.91, 128.15, 128.60, 128.75, 129.64, 136.83, 142.33, 149.99, 161.99 (C=O), 165.04 (C=O). Anal. Calcd for $C_{23}H_{21}N_3O_3$: C 71.30, H 5.46, N 10.85. Found: C 71.07, H 5.42, N 10.92 %.

***N*-{4-[2-(Furan-2-ylmethylene)hydrazinecarbonyl]phenyl}-4-methoxybenzamide (3q)**

Yield: 85%, M.p. = 279°C, FTIR (ν, cm^{-1}): 3304, 3234 (N-H), 3016 (=C-H), 2887 (C-H), 1641 (C=O), 1602 (C=N), 1521, 1494 (C=C), 840 (=C-H). ^{1}H-NMR (400 MHz, DMSO-d_6, ppm): δ 3.85 (s, 3H, OCH_3), 6.64–8.01 (m, 11H, Ar-H), 8.34 (s, 1H, =CH-), 10.36 (s, 1H, -CONH-), 11.73 (s, 1H, -CONHN=). ^{13}C-NMR (100 MHz, DMSO-d_6, ppm): δ 55.36 (OCH_3), 112.09, 113.20, 113.56, 119.32, 126.47, 127.60, 128.27, 129.66, 137.02, 142.51, 145.01, 149.43, 162.01, 162.38 (C=O), 165.08 (C=O). Anal. Calcd for $C_{20}H_{17}N_3O_4$: C 66.11, H 4.72, N 11.56. Found: C 66.26, H 4.77, N 11.48 %.

***N*-{4-[2-(4-Methoxybenzylidene)hydrazinecarbonyl]phenyl}-4-methoxybenzamide (3r)**

Yield: 74%, M.p. = 295 °C. Ref. lit. M.p= 298 °C.[20]

***N*-{4-[2-(3-Fluorobenzylidene)hydrazinecarbonyl]phenyl}-4-methoxybenzamide (3s)**

Yield: 83%, M.p. = 286°C, FTIR (ν, cm^{-1}): 3333, 3255 (N-H), 3037 (=C-H), 2964 (C-H), 1645 (C=O), 1602 (C=N), 1575, 1537 (C=C), 840 (=C-H). ^{1}H-NMR (400 MHz, DMSO-d_6, ppm): δ 3.82 (s, 3H, OCH_3), 7.04–8.00 (m, 12H, Ar-H), 8.46 (s, 1H, =CH-), 10.35 (s, 1H, -CONH-), 11.89 (s, 1H, -CONHN=). ^{13}C-NMR (100 MHz, DMSO-d_6, ppm): δ 55.36 (OCH_3), 112.74, 112.96, 113.57, 116.52, 119.33, 123.30, 126.48, 127.51, 128.37, 129.67, 130.78, 136.89, 142.61, 145.82, 161.12, 162.02, 162.57, 163.54 (C=O), 165.10 (C=O). Anal. Calcd for $C_{22}H_{18}FN_3O_3$: C 67.51, H 4.64, N 10.74. Found: C 67.33, H 4.60, N 10.79%.

***N*-{4-[2-(4-Cyanobenzylidene)hydrazinecarbonyl]phenyl}-4-methoxybenzamide (3t)**

Yield: 68%, M.p. = 306°C, FTIR (ν, cm^{-1}): 3338, 3253 (N-H), 3070 (=C-H), 2978 (C-H), 1645 (C=O), 1600 (C=N), 1539, 1494 (C=C), 839 (=C-H). ^{1}H-NMR (400 MHz, DMSO-d_6, ppm): δ 3.86 (s, 3H, OCH_3), 7.08–8.02 (m, 12H, Ar-H), 8.52 (s, 1H, =CH-), 10.38 (s, 1H, -CONH-), 12.04 (s, 1H, -CONHN=). ^{13}C-NMR (100 MHz, DMSO-d_6, ppm): δ 55.36 (OCH_3), 111.66, 113.57, 118.59, 119.33, 126.45, 127.47, 128.43, 129.67, 132.66, 138.81, 142.71, 145.18, 162.03, 162.62 (C=O), 165.10 (C=O). Anal. Calcd for $C_{23}H_{18}N_4O_3$: C 69.34, H 4.55, N 14.06. Found: C 69.15, H 4.53, N 14.19 %.

***N*-{4-[2-(4-Bromobenzylidene)hydrazinecarbonyl]phenyl}-4-methoxybenzamide (3u)**

Yield: 65%, M.p. = 312-313°C. Ref. lit. M.p= 316°C.[18]

2. 2. Biological activity

2. 2. 1. MTT assay

Cytotoxicity tests of the synthesized compounds were performed in a human prostate cancer cell line (PC-3, ATCC CRL-1435), human breast cancer cell line (MCF-7, ATCC-HTB-22), human colon cancer cell line (HT-29, ATCC-HBT-38) and human umbilical vein endothelial cells (HUVEC, ATCC-CRL-1730). MCF-7 and HT-29 cells were cultured in DMEM medium, PC-3 cells were cultured in RPMI-1640 medium and HUVEC cells were cultured in F-12K medium supplemented with 10% fetal bovine serum FBS), 100 U/mL penicillin and 100 µg/mL streptomycin and 2 mM L-glutamine. The cells were incubated at 37°C in a humidified atmosphere with 5% CO_2. Cells were seeded in 96 well plates at a density of $1x10^4$ and treated with compounds synthesized in different (0.1-1000 µM) concentration ranges. We prepare a 10 mM main stock, dilute them with DMSO and add not exceeding the highest concentration of DMSO (0.5%) (for example, 1 mg compound can be dissolved in about 500 µL DMSO). The compounds we put in the medium are added by dilution in the cell medium when necessary so that they do not exceed the DMSO limit. Paclitaxel was used at the same concentrations as a positive control. The MTT test was performed after the cells were incubated with the synthesized compounds for 24 hours. After incubation, cells were washed once with PBS, and a fresh medium was added. Then, 10 µL of MTT dye (0.5 mg/mL) was placed in each well of the plate and incubated at 37 °C for 4 hours. Finally, DMSO was added and incubated for 30 minutes to dissolve the formazan crystals. Color changes were measured at a wavelength of 570 nm. IC_{50} values were analyzed using the Graphpad Prism 7.00 program. All experiments were performed with triple biological replicates, and data were given as mean±standard deviation.

2. 2. 2. AO/EB Staining

MCF-7, PC-3 and HT-29 cells were seeded in 12 well plates and were incubated with the compound **3h** (IC_{50} concentration) for 24 hours.[21] After incubation, PBS washed cells and incubated them with AO/EB staining solution (100 µg/ml acridine orange and 100 µg/mL ethidium bromide) in PBS. Images of cells were taken under an inverted fluorescent microscope (Zeiss AxioVert1, Germany). In the analysis, green staining shows viable cells, and red staining shows dead or destructed cells, so the intensity was calculated by taking the green/red ratio. All experiments were performed with triple biological replicates, and data were given as mean±standard deviation.

2. 2. 3. Annexin-V assay

MCF-7, PC-3 and HT-29 cells were seeded in 6 well plates. After the cells reached a density of 1×10^6, they were incubated with compound **3h** (IC_{50} concentration) for 24

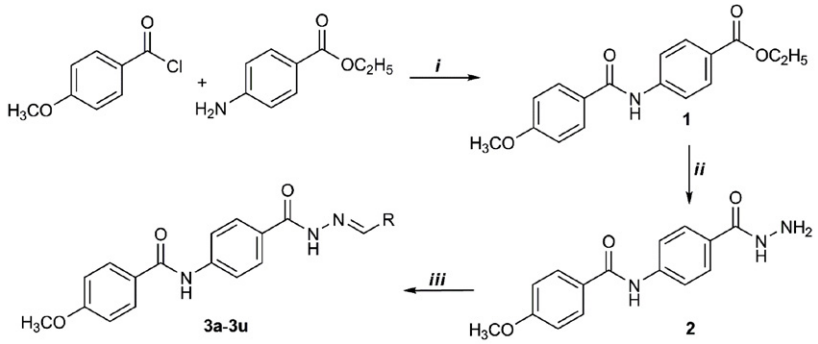

Scheme 1. The synthetic pathways of target compounds. Reagents: (i) ether, 25 °C, 2h, yield: 75%; (ii) hydrazine monohydrate, ethanol, 100 °C, 10h, yield: 80%; (iii) substituted aldehydes, ethanol, reflux, 8h, yield: 57–85%.

hours.[22] After the incubation period was complete, the cells were washed with PBS and removed using trypsin-EDTA. Cells were centrifuged at 600xg for 5 minutes and washed once with PBS. Cells were suspended with a fresh medium containing 10% FBS and performed according to the manufacturer's protocol using the Annexin V & Dead Cell Assay kit (Muse-MCH100105, MilliporeSigma, CA, USA). Cells were incubated in the dark for 30 minutes with the binding buffer and dyes in the kit. Assay results were measured using the Muse Cell Analyzer. All experiments were performed with triple biological replicates, and data were given as mean±standard deviation.

2. 2. 4. Caspase-3 activity

MCF-7, PC-3, and HT-29 cells were seeded in 12 well plates. Cells were incubated with compound **3h** (IC_{50} concentration) for 24 hours and then washed with PBS. Caspase-3 activity in cells was performed using a commercial kit (CASP-3-C, Sigma-Aldrich). After the cells were treated with 100 µl of cell lysis buffer, they were centrifuged at 10.000xg for 10 minutes at 4°C. The supernatant was taken, and measurements were made colorimetrically at a wavelength of 405 nm (Epoch, Biotek) using Ac-DEVD-pNA substrate. The results were calculated as µmol pNA/min/mL, and the protein values of the cells were calculated and used as nmol pNA/min/µg protein. All experiments were performed with triple biological replicates, and data were given as mean±standard deviation.

2. 3. *In silico* ADME analysis

Physicochemical, pharmacokinetic and drug-likeness properties of all compounds were predicted through SwissAdme online server (http://www.swissadme.ch/).

3. Results and Discussion

3. 1. Synthesis

In this study, some hydrazide-hydrazone derivatives were synthesized as given in Scheme 1. Firstly, the amide functional group was prepared from the reaction of *ethyl p-aminobenzoate* and *4-methoxybenzoyl chloride* in ether. In the second step, hydrazide structure was obtained by heating *ethyl 4-(4-methoxybenzamido)benzoate* with hydrazine monohydrate in an ethanolic medium. Finally, hydrazone structures were successfully synthesized by the treatment with hydrazide and different substituted aldehydes in ethanol. The structures of the hydrazone derivatives were elucidated by FTIR, ^{1}H-NMR, and ^{13}C-NMR spectroscopic methods and elemental analysis.

IR spectra of hydrazone compounds (**3a**-**3u**), the C=O stretching bands of compounds were observed at 1637-1653 cm^{-1}. The NH stretching bands of amide and hydrazone structures were detected at 3173-3340 cm^{-1}. The characteristic strong band in the 1600–1606 cm^{-1} region, attributed to a C=N stretching, confirmed the hydrazone feature of all derivatives. In the ^{1}H-NMR spectra, the NH peak of amide structure gave a peak between 10.28 ppm and 10.41 ppm as a singlet. The proton of the imine (-N=CH-) group resonated at 8.33–8.94 ppm as a singlet. The proton of the –CONHN= group was detected at 11.47-12.26 ppm as a singlet. In addition, the disappearance of the proton peaks of the hydrazide amino group is evidence of hydrazone synthesis. In the ^{13}C-NMR spectra, carbonyl peaks were observed at 161.99-165.63 ppm. The carbon of the imine (-N=CH-) group was detected at 144.52-149.99 ppm.

3. 2. Biological activity

The cytotoxicity studies of synthesized compounds were performed on prostate cancer cell line (PC-3), breast cancer cell line (MCF-7), colon cancer cell line (HT-29), and human umbilical vein endothelial cells (HUVEC) compared to the Paclitaxel as a standard compound (Table 1).

Compounds carrying 4-nitrophenyl (**3c**), phenyl (**3l**), benzyl (**3p**), 4-bromophenyl (**3u**) and 3-pyrrole (**3h**) against the PC3 cancer cell line; compounds carrying 4-nitrophenyl (**3c**), 5-nitro-2-furyl (**3j**), 4-hydroxyphenyl (**3m**), benzyl (**3p**), 2-furyl (**3q**) and 3-pyrrole (**3h**) against the MCF-7 cancer cell line; compounds carrying 3-nitrophenyl (**3d**), 2-furyl (**3q**) and 3-pyrrole (**3h**) structures against the HT-29 cancer cell line exhibited significant cytotoxic activity.

Table 1. The IC_{50} values of synthesized compounds.

Comp.	R	PC-3*	MCF-7*	HT-29*	HUVEC*
3a	2,4-dichlorophenyl	137.2±1.2	210.4±12.4	174.2±8.0	218.0±9.1
3b	3,4-(dichloro)phenyl	204.7±0.1	112.3±8.2	102.5±6.7	213.8±8.6
3c	4-nitrophenyl	42.2±1.3	30.1±6.0	54.2±4.0	65.8±5.2
3d	3-nitrophenyl	67.7±2.1	61.0±3.2	36.3±2.9	206.3±1.1
3e	2-hydroxy-3,5-(dichloro)phenyl	81.3±1.1	74.1±2.1	91.0±3.5	154.2±7.3
3f	pyridin-4-yl	178.6±6.3	128.3±7.2	94.2±2.1	302.6±4.1
3g	pyridin-3-yl	321.2±11.0	216.4±9.1	300.1±11.1	314.5±6.1
3h	pyrrol-3-yl	1.3±0.1	3.0±0.1	1.7±0.2	235.3±6.5
3i	thiophen-2-yl	86.4±0.6	165.4±6.0	143.5±3.9	330.3±12.0
3j	5-nitro-2-furyl	88.9±4.1	23.7±3.2	78.2±2.1	538.1±14.7
3k	2-chloroquinolin-3-yl	194.3±3.5	128.2±2.1	205.4±8.7	337.4±4.2
3l	phenyl	46.2±1.0	58.4±5.0	69.1±5.0	84.3±6.0
3m	4-hydroxyphenyl	66.9±6.4	27.1±3.9	86.2±2.2	70.6±3.4
3n	4-hydroxy-3-methoxyphenyl	200.3±8.1	111.1±8.7	170.6±3.1	248.5±8.0
3o	3-(4-chlorophenoxy)phenyl	218.4±9.4	154.1±7.3	204.3±4.6	407.1±11.0
3p	benzyl	14.0±2.0	26.3±2.1	56.1±2.0	67.1±3.3
3q	2-furyl	78.24±8.6	32.2±1.4	44.1±4.2	74.3±2.1
3r	4-methoxyphenyl	103.0±11.1	100.2±5.1	115.4±9.5	233.5±10.9
3s	3-fluorophenyl	258.3±4.0	301.2±12.1	195.3±8.4	374.2±8.7
3t	4-cyanophenyl	145.4±8.0	162.0±4.3	184.1±2.2	388.6±6.2
3u	4-bromophenyl	49.0±5.0	79.2±4.1	62.1±4.3	54.7±1.1
	Paclitaxel	2.4±1.4	5.5±1.1	12.0±2.1	74.4±3.5

*:μM, mean±SD

In particular, the compound having the 3-pyrrole ring (**3h**) was found to have higher cytotoxicity against all cancer cell lines than the standard compound. In addition, the toxicity of this compound against HUVEC is very low. The selectivity index (SI = IC_{50} for normal cell line HUVEC/IC_{50} for cancerous cell line) of compound **3h** was found at 181.0 for PC3, 78.4 for MCF-7, and 138.4 for HT-29. As a result, the compound **3h** has been detected that has a selective cytotoxic effect against cancer cell lines.

While synthesizing the hydrazone structure in order to compare the structure-activity relationship; different aromatic and heteroaromatic rings were selected. The ability of electron-donating or electron-withdrawing groups at different positions on these rings to affect the interactions with cancer cells was also investigated. Among the compounds carrying nitro group, compound **3c** showed high cytotoxic effect against PC3 and MCF7, compound **3d** against HT29, and compound **3j** against MCF7 due to the strong electron withdrawing and resonance properties of the nitro group. Moreover, of these compounds, **3j** showed the least cytotoxic activity against HUVEC normal cell. Many studies showed that that the nitro group has high antiproliferative activity. Nitro compounds can release NO due to redox reactions inside the cell. For these reasons, cytotoxic effects occur due to disruption of oxidative stress mechanisms. Nitro substituents can also increase the inhibition of target biomolecules such as proteins or enzymes due to its electron withdrawing property favoring interaction with some amino acids such as threonine and glutamine. It has been determined that the nitro group of the compounds at the para and meta position shows higher efficiency than the ortho position due to the steric effect.[23, 24]

On the other hand, compound **3h** has a pyrrole ring as a heteroaromatic ring in its structure and showed the highest cytotoxic activity against all cancer cell lines selectively, regardless of the above-mentioned structure-activity relationship.

AO/EB, a dye that allows it to appear under a fluorescent microscope to identify changes in cell membranes during cell death, helps us understand the process of apoptosis. We qualitatively and quantitatively analyzed the changes of compound **3h** (IC_{50} value) on MCF-7, PC-3, and HT-29 cells using the AO/EB staining method. In AO/EB staining of MCF-7 cells, when compound **3h** was compared with the control group, it was observed that the ratio of live cells to dead cells decreased significantly ($p<0.001$, Figure 1a-b). In PC3 cells, compound **3h** was compared with the control group, and it was seen that the viable/dead (green/red) ratio of the cells decreased significantly ($p<0.001$, Figure 2a-b). Finally, in HT-29 cells, the viable/dead ratio of cells in the compound **3h** group was significantly reduced ($p<0.001$, Figure 3a-b).

Annexin-V is a protein that binds to the cell membrane lipid phosphatidylserine from the onset of apoptosis. Annexin-V binding was measured in MCF-7, PC-3, and HT-29 cells after 24 hours of incubation with compound **3h**. In MCF-7 cells, compound **3h** significantly increased the number of cells to early apoptosis, late apoptosis, and dead cells and decreased the number of live cells compared to the control group ($p<0.05$, $p<0.001$, Figure 4a-b). In

PC-3 cells, compound **3h** significantly increased the number of cells going to early apoptosis and late apoptosis, and decreased the number of viable cells compared to the control group ($p<0.05$, $p<0.001$, Figure 5a-b). In HT-29 cells, it was observed that compound **3h** significantly increased only the number of cells going to late apoptosis and decreased the number of viable cells compared to the control group ($p<0.001$, Figure 6a-b).

Caspase-3 is an enzyme that is important in the apoptotic pathway. Caspase-3 is a marker of both intrinsic and extrinsic apoptosis. In the apoptosis of the cell, amino acids in the structure of proteins are targeted by caspase-3 activity, the peptide bonds of the proteins are cut, and the protein that has lost its function cannot perform its function. In this study, caspase-3 activities of compound **3h** were measured enzymatically in MCF-7, PC-3, and HT-29 cells. Compound **3h** increased caspase-3 enzyme activity in MCF-7 cells compared to the control group ($p<0.001$, Figure 4c). In PC-3 cells, compound **3h** increased caspase-3 enzyme activity in 24 hours ($p<0.001$, Figure 5c). Similarly, compound **3h** increased caspase-3 enzyme activity in HT-29 cells compared to the control group ($p<0.001$, Figure 6c).

In this study, among the synthesized compounds, **3h** bearing pyrrole ring showed the highest cytotoxic activity against different cancer cell lines such as breast, colon and prostate, it did not show cytotoxic activity against human umbilical vein endothelial cells. Therefore, compound **3h**, which can show selective activity against cancer cell lines in this study, was obtained.

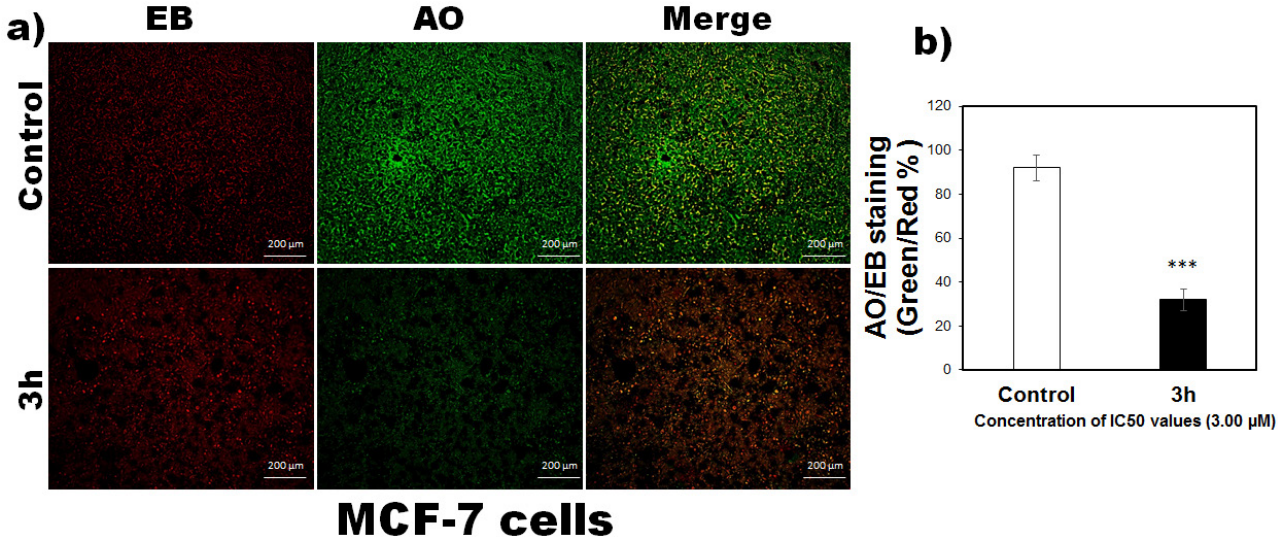

Figure 1. MCF-7 cells treated with 3.00 µM concentration of compound **3h**, **a)** AO/EB staining in floresance imaging **b)** AO/EB staining ratio (*** $p < 0.001$ vs control)

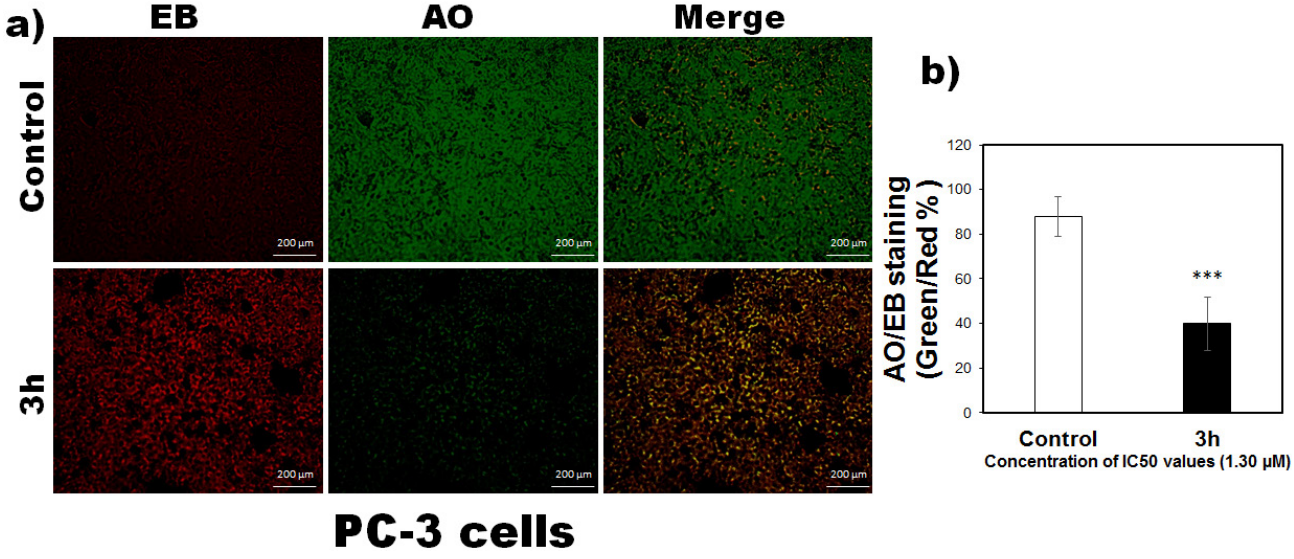

Figure 2. PC-3 cells treated with 1.30 µM concentration of compound **3h**, **a)** AO/EB staining in floresance imaging **b)** AO/EB staining ratio (*** $p < 0.001$ vs control)

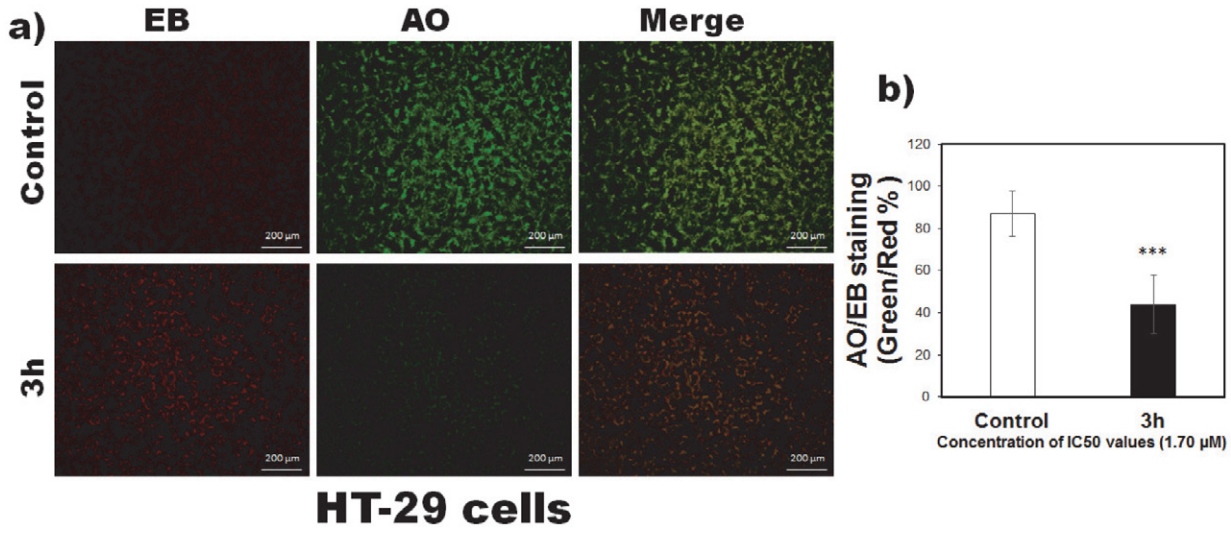

Figure 3. HT-29 cells treated with 1.70 µM concentration of compound **3h**, **a)** AO/EB staining in floresance imaging **b)** AO/EB staining ratio (*** $p < 0.001$ vs control)

In addition to the effectiveness of a compound in the fight against cancer, it is also very important that it exhibits selective activity. There are many examples in the literature where the non-selective compound showing activity against the cancer cell line was not included in further studies.[25,26] Pena-Moran et al. reported that the compound with an SI value ≥ 10 belongs to a selected potential compound that can be investigated further.[27] On the other hand, Weerapreeyakul et al. suggested a lower SI value (≥ 3) for classification of a possible anti-cancer compound.[28]

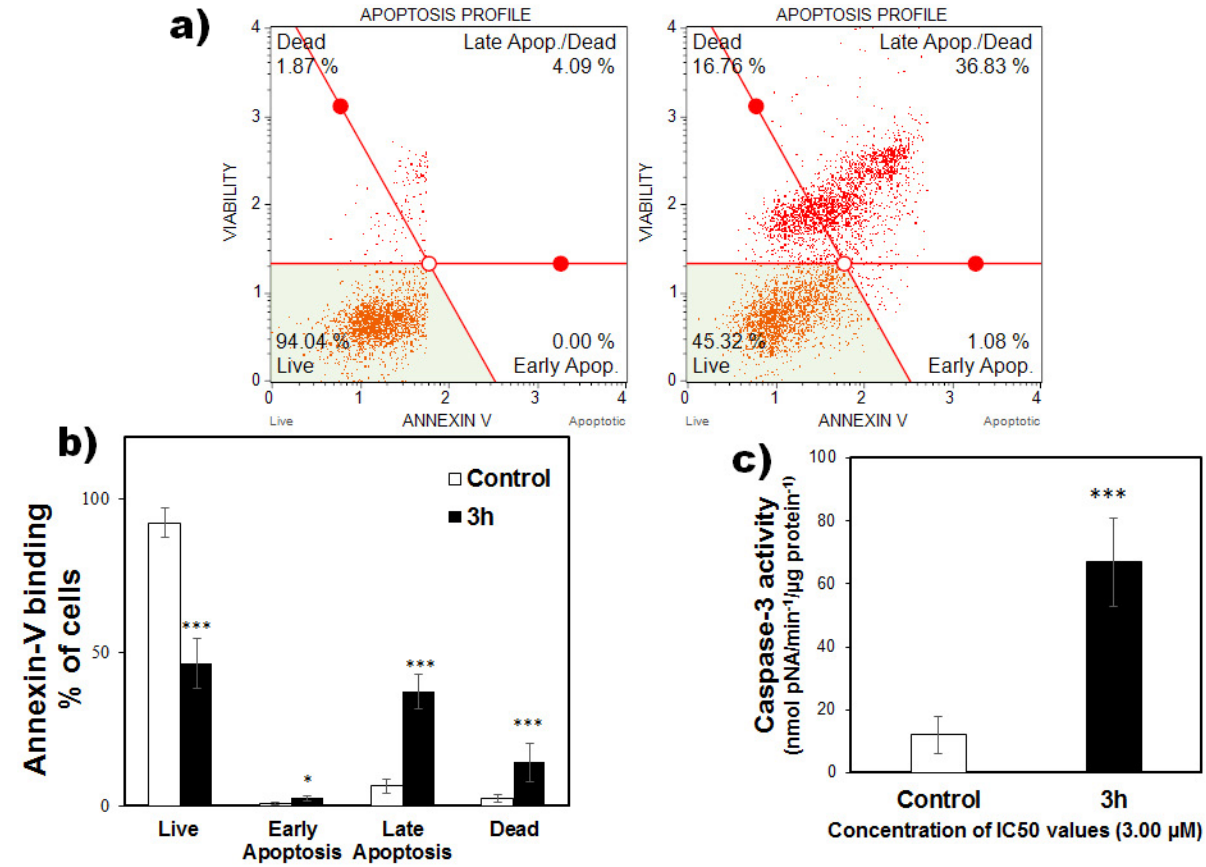

Figure 4. Apoptosis profile for MCF-7 cells treated with compound **3h** (3.00 µM) **a)** Annexin-V binding **b)** The percentage of live, early and late apoptosis/dead cells by MUSE cell analyzer **c)** Caspase-3 activity (* $p < 0.05$, *** $p < 0.001$ vs control)

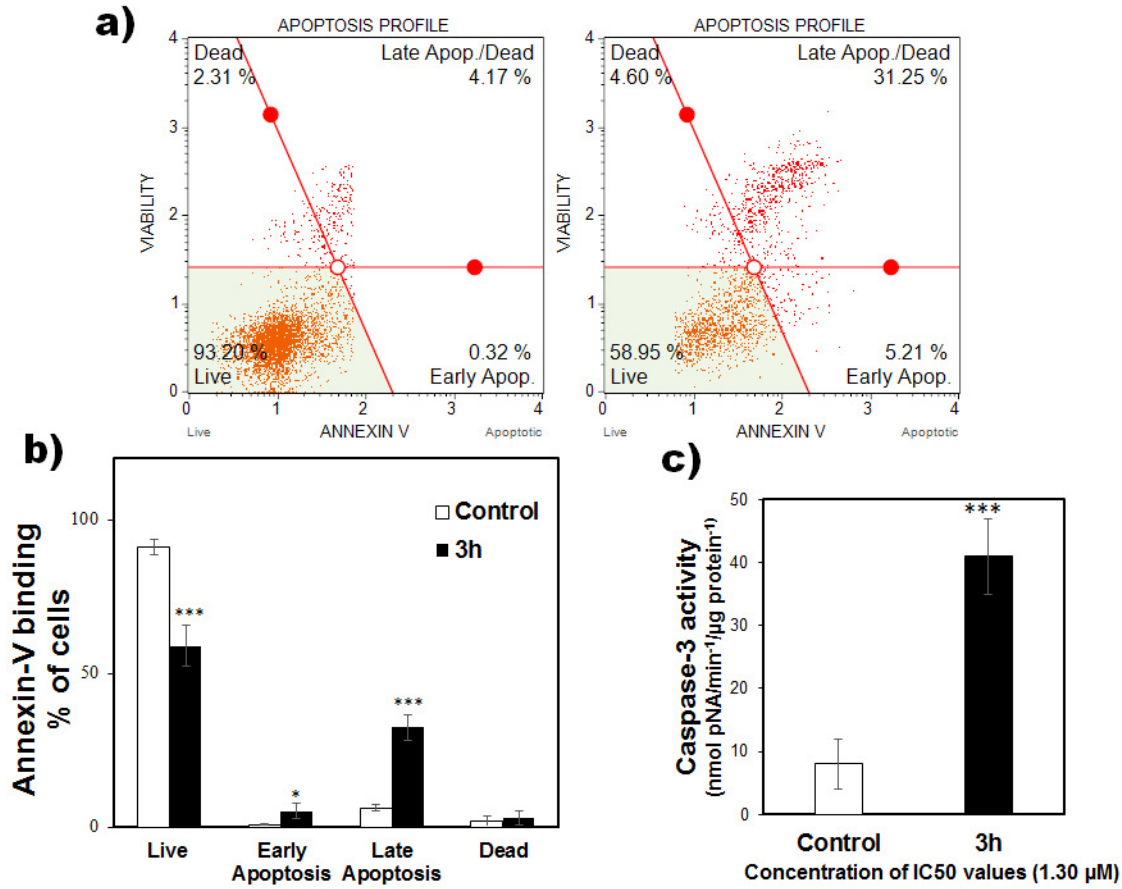

Figure 5. Apoptosis profile for PC-3 cells treated with compound **3h** (1.30 µM) **a)** Annexin-V binding **b)** The percentage of live, early and late apoptosis/dead cells by MUSE cell analyzer **c)** Caspase-3 activity (* $p < 0.05$, *** $p < 0.001$ vs control)

Evaluation of the anti-cancer activity of a compound using only malignant cell lines without SI determination has been reported to be a poor predictor for further (clinical) study.[29] For example colchicine exhibits very high cytotoxic effects. Unfortunately, colchicine is too toxic to be used as an antitumor agent.[30]

As a result, the selectivity index of compound **3h** was found at 181.0 for PC3, 78.4 for MCF-7, and 138.4 for HT-29. The selectivity index of standard drug (Paclitaxel) was found at 31.0 for PC3, 13.5 for MCF-7, and 6.2 for HT-29. The selectivity index of compound **3h** was higher than standard drug. In addition, caspase-3 activity and Annexin-V assay were performed to explain the activity mechanism of compound **3h**. Dose response curves of five compounds (**3c**, **3d**, **3h**, **3l**, **3p** and **3q**) were also added to the Supporting Information (Figure S1).

3. 3. *In silico* ADME analysis

A promising compound must pass *in silico* analysis before it can be taken up for further studies.[31] Therefore, we evaluated the pharmacokinetics, drug-likeness and physicochemical properties of hydrazone derivatives. The drug-likeness was established based on the physicochemical properties to obtain oral drug candidates.[32] All data for the calculation were shown in Tables 2 and 3.

The SwissAdme web tool allows assessing the probability of a molecule to become an oral drug with respect to bioavailability.

There are five different rule-based filters, also defined below, which can be calculated with the SwissAdme program:[33]

(**i**) Lipinski's rule of five includes molecular weight ≤ 500, MLOGP (lipophilicity) ≤ 4.15, hydrogen bond donors ≤ 5 and hydrogen bond acceptors ≤ 10.

(**ii**) Ghose's filter includes 160 ≤ molecular weight ≤ 480, −0.4 ≤ WLOGP (lipophilicity) ≤ 5.6, 40 ≤ the molar refractivity ≤ 130, and 20 ≤ number of atoms ≤ 70.

(**iii**) Veber's rule includes the number of rotatable bonds ≤ 10 and the total polar surface area ≤ 140.

(**iv**) Egan's filter includes WLOGP (Lipophilicity) ≤ 5.88 and the total polar surface area ≤ 131.6.

(**v**) Muegge's filter includes 200 ≤ molecular weight ≤ 600, −2 ≤ XLOGP (lipophilicity) ≤ 5, the total polar surface area ≤ 150, the number of rings ≤ 7, the number of carbon > 4, the number of heteroatoms > 1, the number of rotatable bonds ≤15, the hydrogen bond acceptors ≤ 10, and the hydrogen bond donors ≤ 5.

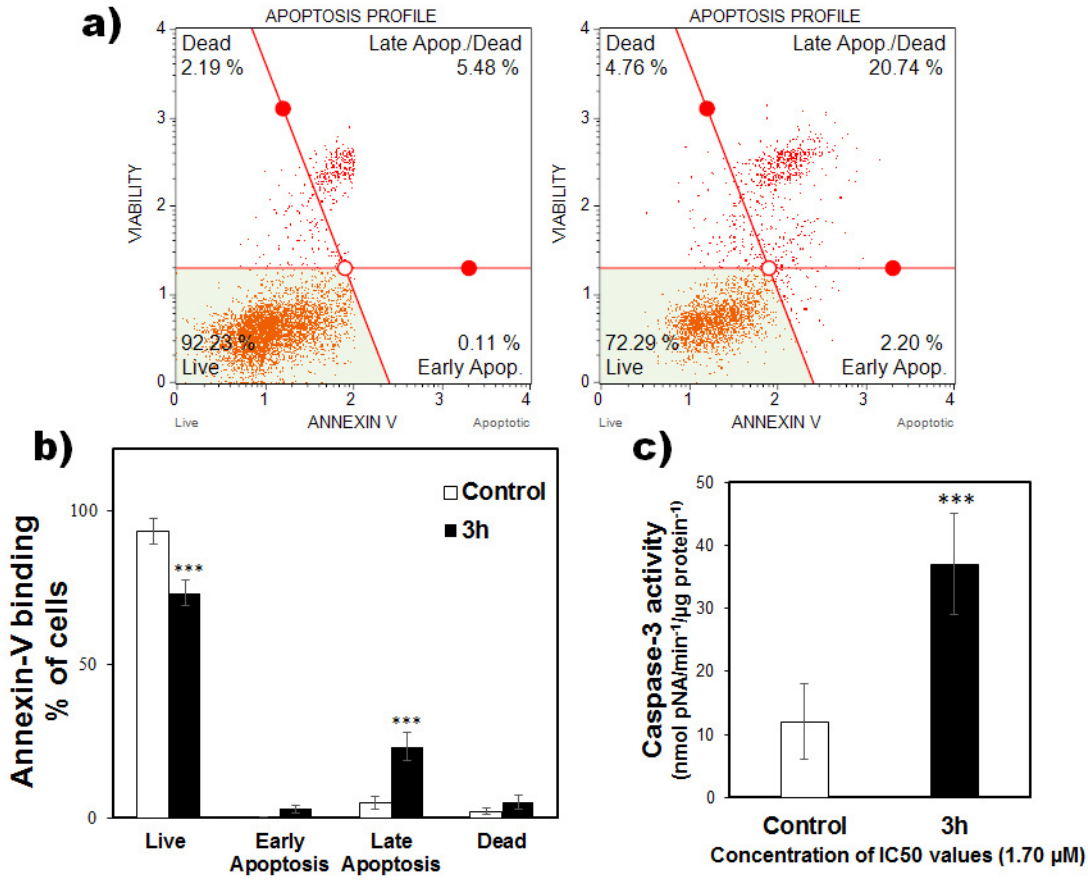

Figure 6. Apoptosis profile for HT-29 cells treated with compound **3h** (1.70 µM) **a)** Annexin-V binding **b)** The percentage of live, early and late apoptosis/dead cells by MUSE cell analyzer **c)** Caspase-3 activity (*** $p < 0.001$ vs control)

The result of the drug-likeness evaluation of hydrazones (**3a**–**u**) was shown in Table 3, and we can conclude that: (**i**) Lipinski, Veber, Ghose, Egan and Muegge filters of all compounds were within the accepted range except compounds **3j** and **3o**. (**ii**) The bioavailability score is 0.55 for all compounds, meaning good bioavailability.

On the other hand, solubility is an another important property related to drug absorption by assessing whether the drug is soluble or moderately soluble. Furthermore, one of the prerequisites for the compound to show activity is that it should have good solubility. Solubility class can be estimated according to the following log S scale: insoluble <−10 <poorly <−6 <moderately <−4 <soluble <−2 <very <0 <highly. Only **3o** of the compounds have poor solubility due to carrying the large lipophilic group (4-chlorophenoxy moiety). It is known that as the number of aromatic rings increases, the solubility decreases.[34] All other compounds were detected to have soluble or moderately soluble. In addition, according to Yalkowsky's general solubility equation, the following relationship can be established between solubility, partition coefficient and melting point.[35] [Log S = 0.5–0.01x(M.P.-25) – Log P]. As a matter of fact, the compound **3o** with the highest partition coefficient (Log P=4.40) has the lowest solubility (Log S = –6.42).

The BOILED-Egg model is used to predict the pharmacokinetic properties of compounds. While molecules in the yellow region easily pass the blood-brain barrier; the white area indicates molecules that pass easily through the gastrointestinal membranes. The absorption of molecules in the gray area is low.[36] The BOILED-Egg model showed that all molecules were in the white region except **3j**, so their absorptions through the gastrointestinal membranes were high. The absence of molecules in the yellow region was important to avoid central side effects (Figure 7). Among the compounds **3h**, having the highest activity, showed agreement with all filters and good gastrointestinal absorption.

4. Conclusion

Cancer is an important public health problem globally. In many medical research projects, the aim is related to the discovery of new safer more effective and selective anticancer agents. Therefore, some hydrazide-hydrazone derivatives were synthesized and investigated for their anticancer potency against carcinogenic PC-3, MCF-7, HT-29 and normal HUVEC cell lines. Among these compounds, **3h** having the 3-pyrrole ring showed more cytotoxic effects against three cancer cell lines than the stand-

ard compound paclitaxel. In addition, this compound did not show any cytotoxic effects against normal endothelial cells. The molecular mechanism revealed that compound **3h** increased the activation of caspase-3 cascade and apoptosis. Moreover, it has good pharmacokinetics and drug-likeness properties. All results suggest that compound **3h** could be a lead compound for the anticancer drug discovery field.

Table 2. The physicochemical properties of hydrazone derivatives (**3a**-**u**).

Comp	MW	FCsp3	*n*-ROTB	*n*-ON	*n*-OHNH	MR	TPSA	cLog P	Log S
3a	442.29	0.05	8	4	2	118.34	79.79	4.13	–5.58
3b	442.29	0.05	8	4	2	118.34	79.79	4.13	–5.58
3c	418.40	0.05	9	6	2	117.14	125.61	2.22	–4.46
3d	418.40	0.05	9	6	2	117.14	125.61	2.22	–4.46
3e	458.29	0.05	8	5	3	120.36	100.02	3.60	–5.44
3f	374.39	0.05	8	5	2	106.11	92.68	1.76	–3.73
3g	374.39	0.05	8	5	2	106.11	92.68	1.76	–3.73
3h	362.38	0.05	8	4	3	102.67	95.58	1.58	–3.56
3i	379.43	0.05	8	4	2	106.19	108.03	2.37	–4.43
3j	408.36	0.05	9	7	2	109.40	138.75	1.47	–4.26
3k	458.90	0.04	8	5	2	128.63	92.68	3.18	–5.72
3l	373.40	0.05	8	4	2	108.32	79.79	3.17	–4.23
3m	389.40	0.05	8	5	3	110.34	100.02	2.64	–4.25
3n	419.43	0.09	9	6	3	116.83	109.25	2.34	–4.32
3o	499.94	0.04	10	5	2	139.84	89.02	4.40	–6.42
3p	387.43	0.09	9	4	2	113.12	79.79	3.39	–4.36
3q	363.37	0.05	8	5	2	100.58	92.93	1.58	–4.30
3r	403.43	0.09	9	5	2	114.81	89.02	2.86	–4.47
3s	391.40	0.05	8	5	2	108.27	79.79	3.55	–4.55
3t	398.41	0.04	8	5	2	113.03	103.58	2.52	–4.34
3u	452.30	0.05	8	4	2	116.02	79.79	3.76	–5.30

MW: Molecular weight, **FCsp3**: Fraction Csp3, ***n*-ROTB:** Number of rotatable bonds, ***n*-ON**: Number of hydrogen bond acceptors, ***n*-OHNH**: Number of hydrogen bond donors, **MR**: Molar Refractivity, **TPSA**: Topological polar surface area, **cLog P**: Partition coefficient and Log S: Water solubility.

Table 3. The drug-likeness and pharmacokinetic properties of target compounds (**3a**-**u**).

Comp	Pharmacokinetics		Druglikeness					
	GI abs.	BBB per.	Lipinski	Veber	Ghose	Egan	Muegge	Bio. score
3a	High	No	√	√	√	√	√	0.55
3b	High	No	√	√	√	√	√	0.55
3c	High	No	√	√	√	√	√	0.55
3d	High	No	√	√	√	√	√	0.55
3e	High	No	√	√	√	√	√	0.55
3f	High	No	√	√	√	√	√	0.55
3g	High	No	√	√	√	√	√	0.55
3h	High	No	√	√	√	√	√	0.55
3i	High	No	√	√	√	√	√	0.55
3j	Low	No	√	√	√	–	√	0.55
3k	High	No	√	√	√	√	√	0.55
3l	High	No	√	√	√	√	√	0.55
3m	High	No	√	√	√	√	√	0.55
3n	High	No	√	√	√	√	√	0.55
3o	High	No	√	√	–	–	–	0.55
3p	High	No	√	√	√	√	√	0.55
3q	High	No	√	√	√	√	√	0.55
3r	High	No	√	√	√	√	√	0.55
3s	High	No	√	√	√	√	√	0.55
3t	High	No	√	√	√	√	√	0.55
3u	High	No	√	√	√	√	√	0.55

GI abs.: Gastrointestinal absorption, **BBB per.:**Blood-brain barrier permeation, **Bio.:** Bioavailability

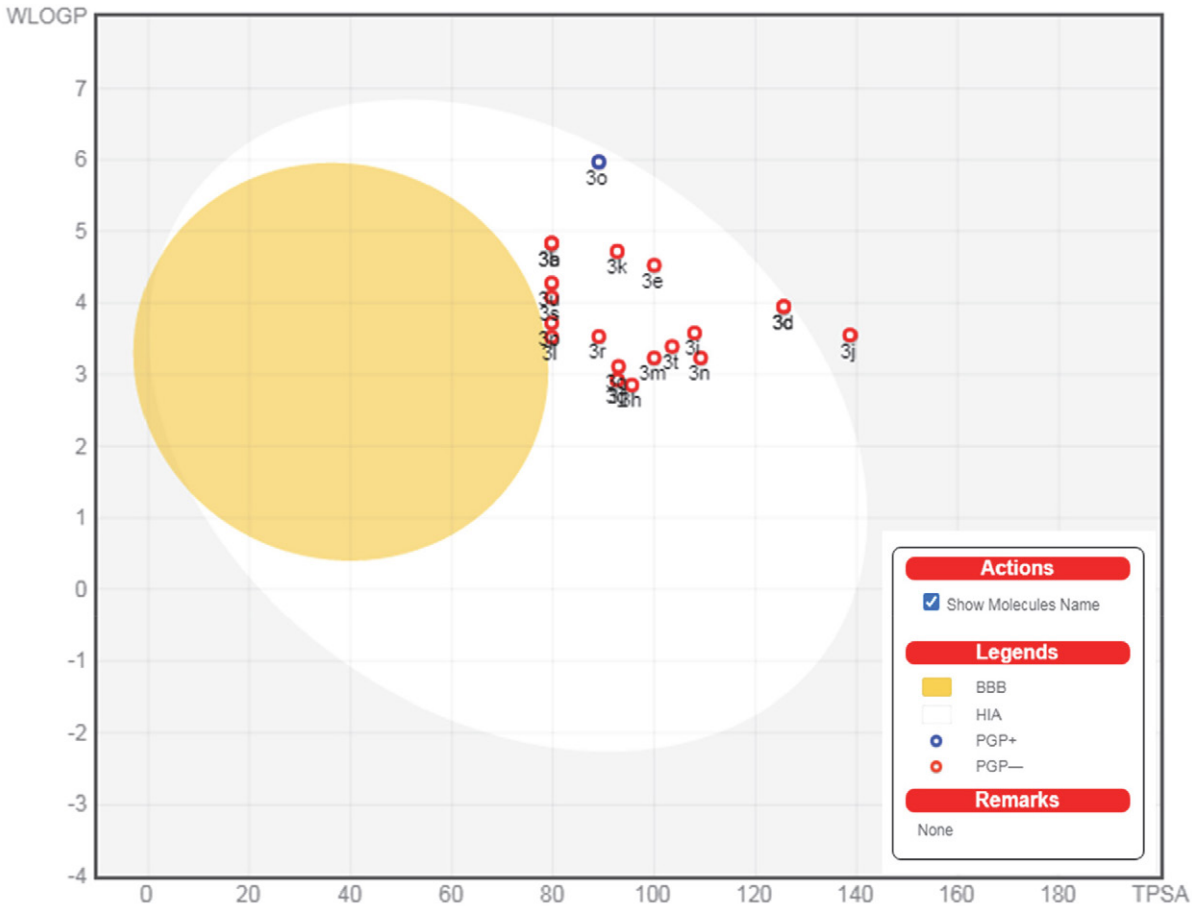

Figure 7. The BOILED-Egg model of target compounds (**3a**-**u**).

Conflict of interest

The authors declare that they have no known competing financial interests.

5. References

1. J. M. Ritter, R. J. Flower, G. Henderson, Y. K. Loke, D. MacEwan, H. P. Rang, Rang & Dale's Pharmacology, 9th edn. Elsevier, China, **2020**.
2. R. Ali, Z. Mırza, G. M. D. Ashraf, M. A. Kamal, S. A. Ansarı, G. A. Damanhourı, A. M. Abuzenadah, A. G. Chaudhary, I. A. Sheıkh, *Anticancer Res.* **2012**, *32(7)*, 2999–3005. **ISSN**: 0250–7005
3. V. Hanusova, L. Skalova, V. Kralova, P. Matouskova, *Curr. Cancer Drug Targets*. **2015**, *15(1)*, 35–52. **DOI:**10.2174/1568009615666141229152812
4. J. Nath, R. Paul, S. K. Ghosh, J. Paul, B. Singha, N. Debnath, *Life Sci*. **2020**, *258*, 1–16. **DOI:**10.1016/j.lfs.2020.118189
5. H. H. Amer, S. H. Alotaibi, A. H. Trawneh, A. M. Metwaly, I. H. Eissa, *Arab. J. Chem*. **2021**, *14*, 1–18. **DOI:**10.1016/j.arabjc.2021.103348
6. A. El-Faham, M. Farooq, S. N. Khattab, N. Abutaha, M. A. Wadaan, H. A. Ghabbour, H. K. Fun, *Molecules*. **2015**, *20*, 14638–14655. **DOI:**10.3390/molecules200814638
7. U. Acar-Çevik, B. N. Sağlık, C. M. Ardıç, Y. Özkay, Ö. Atlı, *Turk. J. Biochem*. **2018**, *43(2)*, 151–158. **DOI:**10.1515/tjb-2017-0167
8. F. Tok, B. N. Sağlık, Y. Özkay, S. Ilgın, Z. A. Kaplancıklı, B. Koçyiğit-Kaymakçıoğlu, *Bioorg. Chem*. **2021**, *114*, 1–11. **DOI:**10.1016/j.bioorg.2021.105038
9. D. Saini, M. Gupta, *Asian J. Pharm. Sci*. **2018**, *4(2)*, 116–122. **DOI:**10.31024/ajpp.2018.4.2.4
10. R. Islam, F. Koizumi, Y. Kodera, K. Inoue, T. Okowara, M. Masutani, *Bioorg. Med. Chem. Lett*. **2014**, *24*, 3802–3806. **DOI:**10.1016/j.bmcl.2014.06.065
11. T. Damghani, F. Moosavi, M. Khoshneviszadeh, M. Mortazavi, S. Pirhadi, Z. Kayani, L. Saso, N. Edraki, O. Firuzi, *Sci. Rep*. **2021**, *11*, 1–20. **DOI:**10.1038/s41598-021-83069-4
12. S. M. Abou-Seri, A. A. M. Eissa, M. G. M. Behery, F. A. Omar, *Bioorg. Chem*. **2021**, *116*, 1–19. **DOI:**10.1016/j.bioorg.2021.105334
13. M. Taha, S. A. A. Shah, M. Afifi, M. Zulkeflee, S. Sultan, A. Wadood, F. Rahim, N. H. Ismail, *Chin. Chem. Lett*. **2017**, *28*, 607–611. **DOI:**10.1016/j.cclet.2016.10.020
14. S. Govindaiah, S. Naha, T. M. Rao, B. C. Revanasiddappa, S. M. Srinivasa, L. Parashuram, S. Velmathi, S. Sreenivasa, *Bioorg. Chem*. **2021**, *3*, 1–14. **DOI:**10.1016/j.rechem.2021.100197

15. S. A. A. Noma, M. Erzengin, T. Tunç, S. Balcıoğlu, *J. Mol. Struct*. **2020**, *1205*, 1–8. **DOI:**10.1016/j.molstruc.2019.127550
16. S. Karakuş, S. Rollas, *J. Res. Pharm*. **2016**, *20(2)*, 199–206. **DOI:**10.12991/mpj.20162013533
17. B. Koçyiğit-Kaymakçıoğlu, S. S. Yazıcı, F. Tok, M. Dikmen, S. Engür, E. E. Oruç-Emre, A. İyidoğan, *Lett. Drug Des. Discov*. **2019**, *16(5)*, 522–532. **DOI:**10.2174/1570180815666180816124102
18. S. G. Kucukguzel, E. E. Oruç, S. Rollas, F. Şahin, A. **Öz**bek, *Eur. J. Med. Chem*. **2002**, *37*, 197–206. **DOI:**10.1016/S0223-5234(01)01326-5
19. N. S. Habib, A. S. Issa, S. M. Rida, F. A. Ashour, G. G. Tawil, *Pharmazie*. **1986**, *41*, 761–764.
20. M. I. Husain, M. Amir, *Curr. Sci*. **1985**, *54(22)*, 1159–1161.
21. Ö. Çevik, D. Li, E. Baljinnyam, D. Manvar, E. M. Pimenta, G. Waris, B. J. Barnes, N. Kaushik-Basu, *J. Biol. Chem. Dec*. **2017**, *292(52)*, 21676–21689. **DOI:**10.1074/jbc.M117.792721
22. Ö. Erdoğan, S. Paşa, G. M. Demirbolat, Ö. Çevik Ö, *Turk. J. Chem*. **2021**, *45(4)*, 1086–1096. **DOI:**10.3906/kim-2102-2
23. S. Noriega, J. Cardoso-Ortiz, A. Lopez-Luna, M. D. R. Cuevas-Flores, J. A. F. D. L. Torre, *Pharmaceuticals*. **2022**, *15(717)*, 1–14. **DOI:**10.3390/ph15060717
24. T. Kauerova, J. Kos, T. Gonec, J. Jampilek, P. Kollar, *Int. J. Mol. Sci*. **2016**, *17(1219)*, 1–14. **DOI:**10.3390/ijms17081219
25. M. Lopez-Lazaro, *Oncoscience*. **2015**, *2(2)*, 91–98. **DOI:**10.18632/oncoscience.132
26. G. Indrayanto, G. S. Putra, F. Suhud, *Profiles Drug Subst. Excip. Relat. Methodol.* **2021**, *46*, 273–307. **DOI:**10.1016/bs.podrm.2020.07.005
27. O. A. Pena-Moran, M. L. Villarreal, L. Alvarez-Berber, A. Meneses-Acosta, V. Rodriguez-Lop, *Molecules*. **2016**, *21(1013)*, 1–15. **DOI:**10.3390/molecules21081013
28. N. Weerapreeyakul, A. Nonpunya, S. Barusrux, T. Thitimetharoch, B. Sripanidkulchai, *Chin. Med*. **2012**, *7(15)*, 1–7. **DOI:**10.1186/1749-8546-7-15
29. M. Lopez-Lazaro, *Drug Discov. Today*. **2015**, *20*, 167–169. **DOI:**10.1016/j.drudis.2014.12.006
30. J. Krzywik, W. Mozga, M. Aminpour, J. Janczak, E. Maj, J. Wietrzyk, J. A. Tuszynski, A. Huczynski, *Molecules*. **2020**, *25(1789)*, 1–33. **DOI:**10.3390/molecules25081789
31. B. N. Sağlık, B. Kaya-Çavuşoğlu, U. Acar-Çevik, D. Osmaniye, S. Levent, Y. Özkay, Z. A. Kaplancıklı, *RSC Med. Chem*. **2020**, *11*, 1063–1074. **DOI:**10.1039/D0MD00150C
32. A. S. Hassan, *J. Iran. Chem. Soc*. **2022**, Accepted paper. **DOI:**10.1007/s13738-022-02551-6
33. S. Pathania, P. K. Singh, *Expert Opin. Drug Metab. Toxicol*. **2021**, *17*, 351–354. **DOI:**10.1080/17425255.2021.1865309
34. S. B. Bunally, C. N. Luscombe, R. J. Young, *SLAS Discov*. **2019**, *24*, 791–801. **DOI:**10.1177/2472555219859845
35. C. P. Tinworth, R. J. Young, *J. Med. Chem*. **2020**, *63*, 10091-10108. **DOI:**10.1021/acs.jmedchem.9b01596
36. F. Tok, B. I. Abas, Ö. Çevik, B. Koçyiğit-Kaymakçıoğlu, *Bioorg. Chem*. **2020**, *102*, 1–10. **DOI:**10.1016/j.bioorg.2020.104063

Povzetek

V raziskavi smo sintetizirali serijo hidrazid-hidrazonskih derivatov (3a-3u) in ocenili njihovo protirakavo delovanje na celično linijo raka prostate (PC-3), celično linijo raka dojke (MCF-7), celično linijo raka debelega črevesa (HT-29) in endotelijske celice človeške popkovnične vene (HUVEC) z uporabo testa MTT. Spojina 3h s pirolnim obročem je predstavljala najmočnejši derivat z IC50 = 1,3; 3,0 in 1,7 μM proti rakavim celicam PC-3, MCF-7 in HT-29, pri čemer je bil kot standardna spojina uporabljen paklitaksel. Poleg tega smo spojino 3h vključili v nadaljnje biološke študije, kot sta aktivnost kaspaze-3 in test aneksina-V, da bi ocenili njen inhibitorni potencial. Rezultati aktivnosti so pokazali, da spojina 3h poveča aktivacijo kaspaze-3 in število celic v zgodnji apoptozi. Izvedene so bile tudi dodatne študije, kot so farmakokinetika, ocena biološke razpoložljivosti in podobnost učinkovinam. Farmakokinetične napovedi *in silico* so pokazale, da bi biološka razpoložljivost teh spojin lahko bila visoka.